Analytical and Bioanalytical Chemistry (2018) 410:7671–7678
https://doi.org/10.1007/s00216-018-1381-3

RESEARCH PAPER

# A novel electrochemical aptasensor based on gold electrode decorated Ag@Au core-shell nanoparticles for sulfamethazine determination

Baoshan He[1] · Ming Li[1]

Received: 11 July 2018 / Revised: 15 August 2018 / Accepted: 14 September 2018 / Published online: 29 October 2018


## Abstract

In this paper, an electrochemical aptasensor based on gold electrode (AuE)-modified Ag@Au core-shell nanoparticles was prepared. The surface of AuE was modified with Ag@Au core-shell nanoparticles to elevate APT binding sites and accelerate electron transfer properties between the electrode and ferrocene (Fc). When $SM_2$ existed, the aptamer conformation would change and the response current intensity would increase because the Fc was pulled closer to the electrode surface. Subsequently, through a series of conditional optimization analysis, the optimal values of volume of Ag@Au core-shell, APT concentration, APT incubation time, and $SM_2$ incubation time were 9 μL, 0.2 μmol/L, 75 min, and 40 min, respectively. Under optimum conditions, the results of differential pulse voltammetry experiments showed that the linear relationship was good in the range of 0.1~50 ng/mL, $\Delta I'$ (μA) = 1.145$C$ (ng/mL) + 54.666, $R^2$ = 0.964, with a detection limit of 0.033 ng/mL. The spiked recovery for $SM_2$ in the pork samples was 92.6~101.0% and the relative standard deviation (RSD) was 2.7~4.1%, which indicated that the proposed aptasensor exhibited desirable performance in actual sample analysis.

**Keywords** Sulfamethazine · Aptasensor · Ag@Au core-shell · Gold electrode · Ferrocene

## Introduction

Sulfonamides (SAs), a kind of antibacterial agents, possess the structure of p-aminophenylsulfonamide (Scheme 1), which have a significant effect in killing bacteria and treating diseases [1–3]. However, due to the nonstandard use of sulfonamides drugs in the prevention and treatment process, many animal-derived foods often have residual problems of such drugs. The excessive residues in food can do harm to human health. For example, it will destroy the balance of normal bacteria of the body and contribute to the problem of pathogenic bacteria resistance [4]. And when the amount of sulfonamide drug residual in the body reaches a certain level, it can also cause teratogenesis, carcinogenesis, and mutagenesis [5]. At present, many countries have set the maximum residue limit of sulfonamides at 100 μg/kg, such as Canada, the USA, and China [6–8].

Numerous methods have been employed to detect sulfonamides in food such as high-performance liquid chromatography (HPLC) [9–11], gas chromatography mass spectrometry (GC-MS) [12, 13], liquid chromatography tandem mass spectrometry (LC-MS/MS) [4, 14, 15], and capillary electrophoresis mass spectrometry (CE-MS) [16, 17]. These methods have been proved to be appropriate and sensitive for SAs detection. Despite all this, some of them are expensive, tedious preparation time and require professionals to operate, which are difficult to meet the need of on-the-spot detection [18].

In recent years, a novel detection method of electrochemical aptasensor is developed, which is also based on the principle of antigen-antibody binding [19]. This method has great potential in the detection of veterinary drug residue with the advantages of easy to operate, less time to analyze, and other advantages of concern [20]. However, there is a common problem with high detection limit. The unique properties of nanomaterials have provided extensive approach for improving the sensitivity of electrochemical aptasensor [21, 22]. A class of nanoparticles, such as Ag, Au, and Pt, were of interest because of their excellent physical and chemical features and were in wide use [23, 24]. Especially, bimetallic nanoparticles

✉ Baoshan He
hebaoshan@126.com

[1] School of Food Science and Technology, Henan Key Laboratory of Cereal and Oil Food Safety Inspection and Control, Henan University of Technology, Lianhua Road 100#, Zhengzhou High & New Technology Industries Development Zone, Zhengzhou 450001, Henan, China

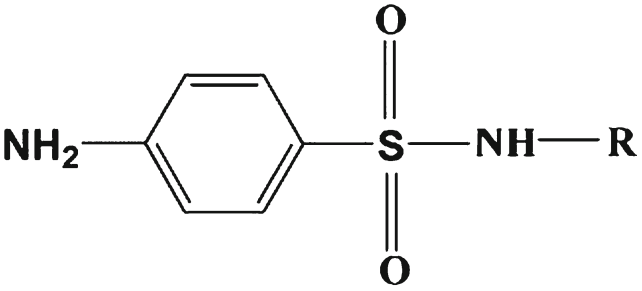


**Scheme 1** Chemical structure of sulfonamides

show synergistic effect and behave better electrocatalytic activity than the single metal nanoparticles with the same elements [25, 26]. Ezat et al. [27] have studied aptasensor constructed by Ag@Au core-shell nanoparticles using *E. coli*, and found that the nanocomposites have high biocompatibility and chemical stability. Li et al. [28] prepared a label-free electrochemical immunosensor using Au@Pd/Ag yolk-bimetallic shell nanoparticles and amination graphene, which presented a relatively wide linear range and low detection limit.

In this paper, we combined Ag@Au core-shell nanoparticles as a sensing platform and thiolated aptamer as a recognition element to construct sensitive aptasensors. Ag@Au core-shell nanoparticles were modified on the AuE surface to increase the effective electrode surface as an immobilization platform for thiolated aptamers and increase electrode sensitivity. The detection mechanism of $SM_2$ was based on current signal produced by Fc before and after incubation. The resulted showed that the MCH/APT/Ag@Au/AuE had good stability, high sensitivity, and good repeatability in the detection of $SM_2$ samples.

## Experimental

### Materials

The experiment involved three sulfonamides (SAs), sulfamethazine ($SM_2$), sulfapyridine (SPD), and sulfanilamide (SHZ) were bought from Aladdin Industrial Co., Ltd. (Shanghai, China). Erythromycin (EM) was purchased from TCL (Shanghai) Development Co., Ltd. Chloroauric acid ($HAuCl_4{\cdot}3H_2O$), 6-mercapto-1-hexanol (MCH), tris (2-carboxyethyl) phosphine (TCEP), nitrofurantoin (NIT), and tris (hydroxymethyl) aminomethane (TRIS) were obtained from yuanye Bio-Technology Co., Ltd. (Shanghai, China). All chemical reagents were used without further processing and purification. Double-distilled water was used throughout the experiment. Ferricyanide ($[Fe(CN)_6]^{3-/4-}$) was used as electron transfer mediator. Tris-HCl buffer solution (10 mmol/L, 1 mmol/L EDTA, pH 7.4) was used as electrolyte in the electrochemical process. And, the standard $SM_2$ solution was prepared with a Tris-HCl buffer solution.

Oligonucleotide designed in this experiment was synthesized by Sangon Biotech Co., Ltd. (Shanghai, China). The aptamer probe sequence is listed as follows: 5′SH-TTA GCT TAT GCG TTG GCC GGG ATA AGG ATC CAG CCG TTG TAG ATT TGC GTT CTA ACT CTC-Fc3′ (APT). Ten millimolar of TCEP solution was prepared by adding 0.0143 g of TCEP to 5 mL of Tris-HCl. The preparation method was to add 17 μL of TCEP solution to per OD primer and made it into 100 μmol/L stock solution. Different concentrations of APT were diluted with Tris-HCl buffer solution and stored at − 20 °C.

### Instruments and measurements

Scanning electron microscope (SEM) was performed using JSM-6700F (Japan Electron Company) operated at 10.00 kV. The UV-vis absorption spectra were collected using a UV-6100s double beam spectrophotometer (Mapada, China). The KQ3200E ultrasonic cleaner was supplied by Kunshan Ultrasonic Instrument Company. Cyclic voltammetry (CV), electrochemical impedance spectroscopy (EIS), and differential pulse voltammogram (DPV) were carried out in a conventional three-electrode system on a CHI660E electrochemical workstation (Shanghai Chen Hua Instrument Company, China). The modified AuE was used as working electrode, an Ag/AgCl electrode as the reference electrode and Pt wire as the counter electrode. All electrochemical experiments were carried out at 25 ± 0.5 °C.

### Preparation of Ag@Au core-shell nanoparticles

Ag@Au core-shell nanoparticles were synthesized according to seed growth method [29, 30]. First, Ag NPs were prepared via the citrate reduction method [31, 32]. For this purpose, 25 mL of 1 mmol/L $AgNO_3$ solution was placed in a 50-mL round flask and stirred with heating at 100 °C in a water bath till reflux achieving. Subsequently, 0.5 mL of a $3.4 \times 10^{-3}$ mmol/L aqueous solution of trisodium citrate was added to the above $AgNO_3$ solution, and after about 30 min of refluxing, it changed from yellow to gray-yellow. Then, centrifuged at 4000 rpm for 30 min, the upper part of dispersion turned transparent yellow. The solution containing Ag NPs was removed with one-time straw and used as core particles. Finally, $HAuCl_4{\cdot}3H_2O$ (5 mL, 0.0831 mmol/L) and trisodium citrate (5 mL, 0.8446 mmol/L) were synchronously introduced to refluxing Ag NPs dispersion. After boiling for 30 min, the yellow solution turned from yellow to slightly orange because of the coating of Au onto the Ag core. The prepared nanoparticles were stored in the refrigerator for further experiments.

### Fabrication of electrochemical aptasensor

In the fabrication process of the aptasensor (Fig. 1), a gold electrode was carefully polished by electric polishing machine with 0.05 μm $Al_2O_3$ powder till mirror surface producing, sonicated in absolute ethanol and double-distilled water for 5 min. Next, the electrode was activated by piranha solution (3:1 $H_2SO_4$ 98%: $H_2O_2$ 25%) for 30 min. After washing with double-distilled water, 10 μL of Ag@Au core-shell nanoparticles solution was dropped onto the AuE surface and dried under infrared light. Three microliters of 0.5 μmol/L aptamer was dropwise added onto the modified electrode and was incubated 1 h at 37 °C. Subsequently, 2 μL of 0.01 mmol/L MCH solution was dropped onto the surface of AuE and was incubated 1 h at 37 °C to eliminate the nonspecific adsorption sites. Ultimately, un-immobilized APT was removed by rinsing with double-distilled water. The fabricated MCH/APT/Ag@Au/AuE was stored at 4 °C when not in use. The detection principle was on the basis of the change of current signal of DPV in Tris-HCl buffer solution before and after incubation of $SM_2$. After the formation of APT-$SM_2$ complex, the ferrocene modified on the aptamer was pulled closer to the electrode surface and sped up the electron transfer rate.

## Result and discussion

### Assessment of the Ag@Au core-shell nanoparticle structure

Figure 2a shows the UV-vis absorption spectra of Ag NPs, Ag@Au core-shell, and Au NPs. The peak wavelengths occurred at 425, 457.2, and 524.5 nm for Ag NPs, Ag@Au core-shell, Au NPs, respectively, which were consistent with the references [31, 33]. And, SEM was utilized to characterize Ag@Au core-shell nanoparticles. As presented in Fig. 2b, the morphological features of Ag@Au core-shell nanoparticles were uniform in shape and quasi-spherical, which were

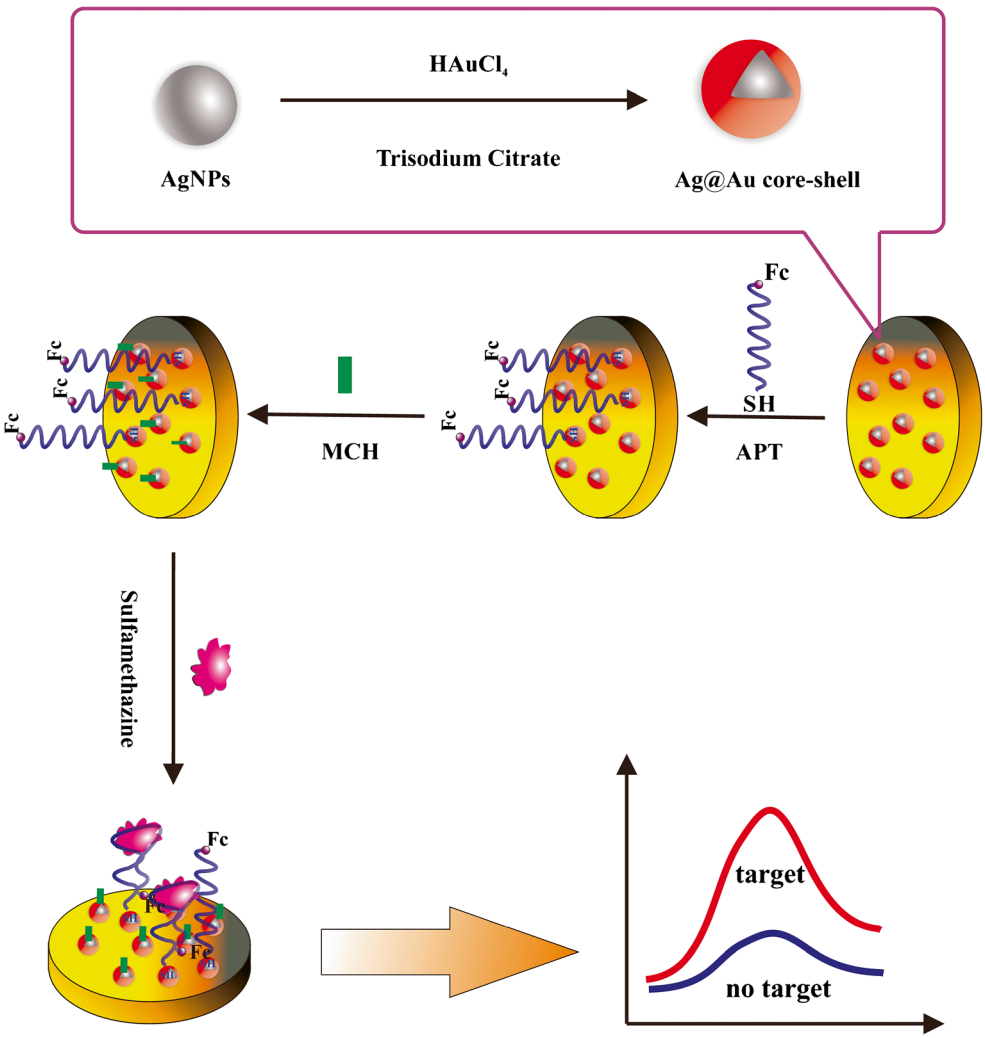


**Fig. 1** Schematic illustration of the electrochemical aptasensor fabrication

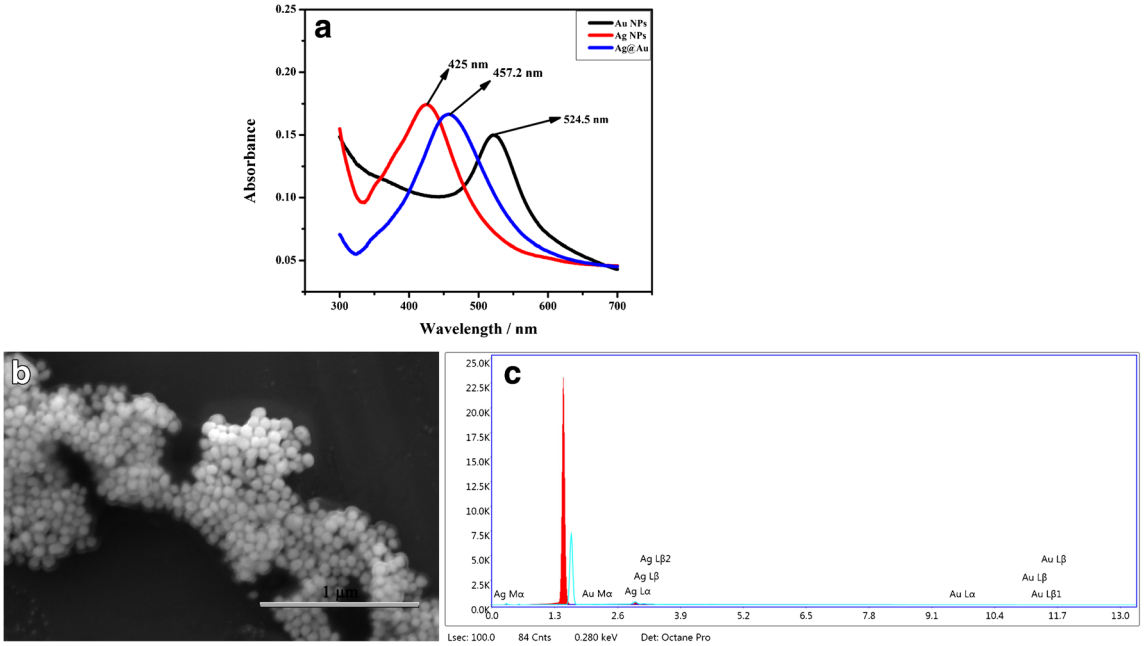


**Fig. 2** (**a**) UV-vis absorption spectra of Ag NPs, Ag@Au core-shell, and Au NPs. (**b**) The SEM image of Ag@Au core-shell nanoparticles. (**c**) EDS elemental analysis spectrum of Ag@Au core-shell

consistent with the results of previous literatures [34]. Beyond that, the EDS measurement of Ag@Au core-shell nanoparticles showed that the prepared sample consisted of Au and Ag atoms (Fig. 2c). Therefore, Ag@Au core-shell nanoparticles were successfully prepared

## Electrochemical characterization of proposed aptasensor

Figure 3 describes typical electrochemical impedance spectroscopy (EIS) obtained at the bare AuE (a), Ag@Au core-shell/AuE (b), APT/Ag@Au core-shell/AuE (c), MCH/APT/Ag@Au core-shell/AuE (d), and $SM_2$/MCH/APT/Ag@Au core-shell/AuE (e) in 5 mmol/L $[Fe(CN)_6]^{3-/4-}$ containing 0.1 mmol/L KCl. The diameter of the small semicircle of the nyquist plots corresponded to the magnitude of the electron transfer resistance (Ret). As shown in Fig. 3, the Nyquist diameter of $[Fe(CN)_6]^{3-/4-}$ on Ag@Au core-shell/AuE (b) (Ret = 30.83 Ω) was lower than that observed on bare AuE (a) (Ret = 82.39 Ω), indicating Ag@Au core-shell could improve electrode conductivity. But, after APT immobilized on Ag@Au core-shell/AuE surface (c), the Ret of electrode was increased (Ret = 58.40 Ω). It was due to the strong electrostatic repulsion interaction between nucleotide bases of aptamer and $[Fe(CN)_6]^{3-/4-}$ [35]. In order to occupy extra binding sites on the AuE surface, the MCH was dropped on the electrode surface and the Ret of electrode increased further (curve *d*, Ret = 215.00 Ω). And after the incubation of aptamer with $SM_2$, the Ret increased to 345.10 Ω. The reasonable explanation was that after the specific binding with $SM_2$, the conformation of the aptamer changed, blocking the electron transfer efficiency.

## Optimization of analytical conditions

To find out the optimal amount of Ag@Au core-shell nanoparticles modified on AuE, the DPV response of six different

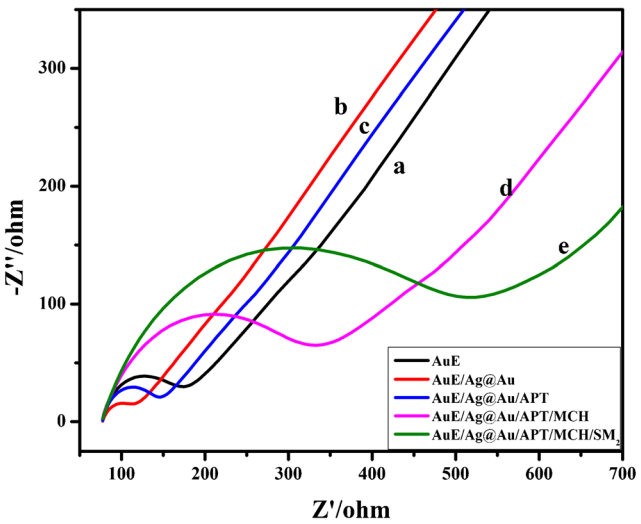


**Fig. 3** EIS of different electrodes recorded in 5 mmol/L $[Fe(CN)_6]^{3-/4-}$ containing 0.1 mol/L KCl ((**a**) bare AuE; (**b**) Ag@Au core-shell/AuE; (**c**) APT/Ag@Au core-shell/AuE; (**d**) MCH/APT/Ag@Au core-shell/AuE; (**e**) $SM_2$/MCH/APT/Ag@Au core-shell/AuE)

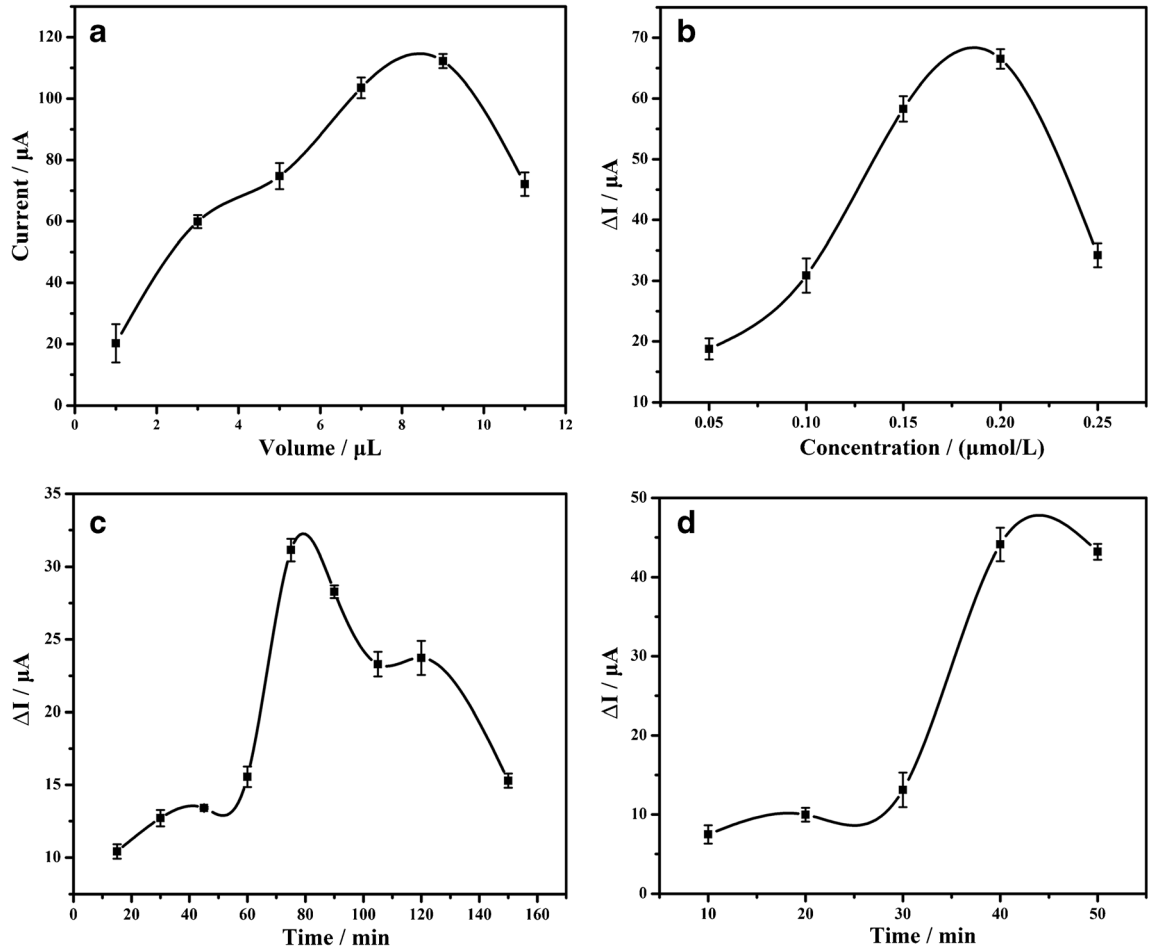


**Fig. 4** Optimization of analytical conditions ((**a**) volume of Ag@Au core-shell; (**b**) $SM_2$ APT concentration; (**c**) APT incubation time; (**d**) $SM_2$ incubation time)

modification amounts (1, 3, 5, 7, 9, 11 μL) on the electrode in 5 mmol/L $[Fe(CN)_6]^{3-/4-}$ (containing 0.1 mol/L KCl) solution was investigated. Figure 4a presents the current signal gradually increased with the amount of Ag@Au core-shell modified on AuE until 9 μL when the current tended to peak. Thus, the optimum amount of Ag@Au core-shell modified on electrode was 9 μL.

Meantime, the aptamer concentration, aptamer incubation time, and target incubation time are also important parameters affecting the property of electrochemical aptasensor. For this

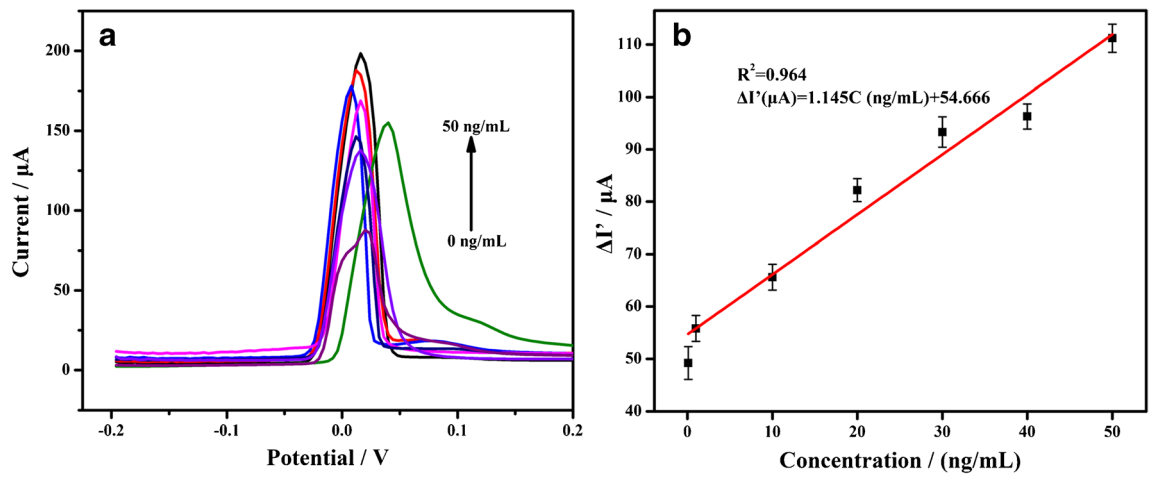


**Fig. 5** (**a**) DPV response of the proposed aptasensor for varying $SM_2$ concentration (0, 0.1, 1.0, 10.0, 20.0, 30.0, 40.0, 50.0 ng/mL). (**b**) Calibration curve of DPV peak currents for different $SM_2$ concentrations

**Table 1** Comparison of the analytical performance of the proposed aptasensor with other analytical methods for the detection of $SM_2$

| Method | Linear range | LOD | References |
|---|---|---|---|
| Enzyme-linked aptamer assay | 0.1–10 ng/mL | 0.05 ng/mL | [36] |
| Electroanalytical assay | 1.0–500 μmol/L | 0.16 μmol/L | [37] |
| High-performance liquid chromatography-chemiluminescence | 1.8–25 μg/mL | 1.50 μg/mL | [9] |
| Electrochemical aptasensor | 0.1–50 ng/mL | 0.033 ng/mL | This work |

purpose, CV was used to measure the changes of current response ($\Delta I$) in a 5 mmol/L $[Fe(CN)_6]^{3-/4-}$ (containing 0.1 mol/L KCl) solution before and after incubation of $SM_2$ to optimize the experimental parameters. As shown in Fig. 4b, $\Delta I$ gradually increased when the concentration was from 0.05 to 0.2 μmol/L and tended to the maximum at the concentration 0.2 μmol/L and decreased in the higher concentration, suggesting that APT immobilized on the electrode was saturated. The effect of APT incubation time had been studied (Fig. 4c). It could be seen, $\Delta I$ reached a maximum at 75 min. Furthermore, incubation time of aptamer in $SM_2$ solution would directly determine the number of APT-$SM_2$ complexes. Different incubation times (10, 20, 30, 40, 50 min) of MCH/APT/Ag@Au/AuE in $SM_2$ solution were investigated. From Fig. 4d, when the target was incubated for 40 min, the surface of the electrode was saturated and the change of current response tended to a maximum. Hence, the optimal values of APT concentration, APT incubation time, and $SM_2$ incubation time were 0.2 μmol/L, 75 min, and 40 min, respectively.

## Evaluation of electrochemical aptasensor

We assessed the electrochemical aptasensor response to different $SM_2$ concentrations by using DPV in Tris-HCl buffer solution. Figure 5a shows the changes of current response ($\Delta I'$) increased gradually with increment of $SM_2$ concentration. Figure 5b indicates that the $\Delta I'$ was proportional to $SM_2$ concentration range from 0.1 to 50 ng/mL. The linear regression equation was $\Delta I'$ (μA) = 1.145$C$ (ng/mL) + 54.666 ($R^2$ = 0.964, $n$ = 3) with the limit detection (LOD) of 0.033 ng/mL. It could be seen that the aptasensor possessed an excellent sensitivity. The reasonable explanation was that the aptamer conformation would change when the $SM_2$ existed, and the Fc was pulled closer to the electrode surface, which accelerated electron transport. Besides, the analytical performance of our method for the detection of $SM_2$ was compared with that of some earlier reported methods (Table 1), demonstrating the superiority of the proposed strategy in this work.

## Selectivity of electrochemical aptasensor

For an excellent electrochemical aptasensor, selectivity was an important index. To evaluate the selectivity of the prepared electrochemical aptasensor, three sulfonamides drugs (50 ng/mL $SM_2$, 50 ng/mL SHZ, and 50 ng/mL SPD) with similar chemical structures were tested. In addition, two antimicrobials (50 ng/mL EM, 50 ng/mL NIT) with absolute different structure were detected using prepared electrochemical aptasensor. Figure 6 shows the changes of current response ($\Delta I'$) of electrochemical aptasensor under optimal experimental conditions. The prepared aptasensor exhibited a much higher $\Delta I'$ in the present of $SM_2$ than other antimicrobials. It could be concluded that the prepared electrochemical aptasensor had relatively high selectivity toward $SM_2$.

## Reproducibility and stability of electrochemical aptasensor

To study the reproducibility of the fabricated electrochemical aptasensor, 10 aptasensors were fabricated for 50 ng/mL $SM_2$ detection. The RSD of 10 parallel tests was below 5%. Meanwhile, the stability of aptasensor was investigated through the same batch aptasensors. These aptasensors were stored at 4 °C in the refrigerator and measured every 1 day. After 1 week, the RSD of $\Delta I'$ of these batch aptasensors was 6.28%. The above results confrmed that the prepared aptasensor possessed good reproducibility and stability.

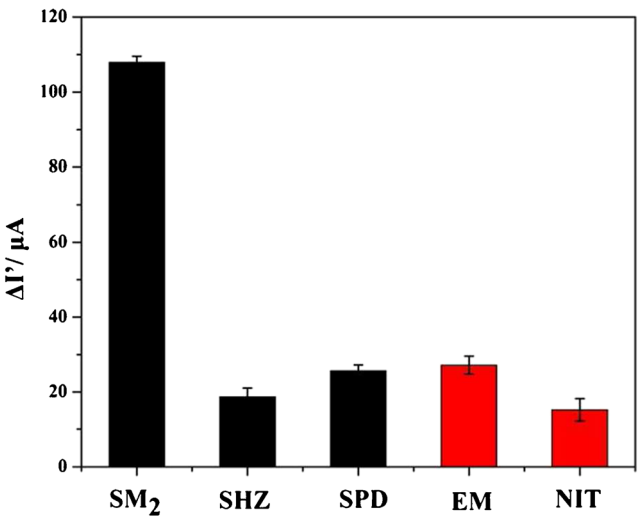


**Fig. 6** Selectivity of electrochemical aptasensor against sulfonamides (black color) and other types of antimicrobials (red color) at 50 ng/mL

**Table 2** Recovery results of aptasensor for detecting $SM_2$ in real samples($n = 3$)

| Sample ($SM_2$) | Added (ng/mL) | Founded (ng/mL) | Recovery (%) | RSD (%, $n = 3$) |
|---|---|---|---|---|
| Pork | 5.0 | 4.63 | 92.6 | 4.1 |
| | 20.0 | 19.08 | 95.4 | 2.7 |
| | 30.0 | 30.33 | 101.0 | 3.5 |

## Analysis of spiked pork samples

The feasibility of this strategy was also demonstrated by detecting the recoveries of different concentrations (5.0, 20.0, 30.0 ng/mL) of $SM_2$ in spiked pork samples. First, 1.0 ± 0.05 g of chopped pork samples (purchased at a local supermarket) was weighed in three centrifugal tubes. Then, 5 mL of a methanol-water mixed solution (*V*:*V* 1:1) was added, homogenized for 1 min, centrifuged at 10,000 r/min for 5 min, and the supernatant was discarded. Two milliliters of 5.0, 20.0, and 30.0 ng/mL of $SM_2$ standard solution was added to the deposit. The mixture was shaken for 1 min, and reacted at 35 °C for 2 h in an incubator. Next, 2 mL of ethyl acetate was added separately, shaken for 10 min, and then centrifuged at 10,000 r/min for 10 min. Finally, the ethyl acetate layer was collected, dried using $N_2$, and the residue was dissolved in Tris-HCl buffer solution to a volume of 2 mL. The recovery for three samples was 92.6~101.0% and the RSD was in the range of 2.7~4.1%. The results were presented in Table 2, indicating that the electrochemical aptasensor was successfully applied to detect $SM_2$ in pork samples.

## Conclusion

In summary, a signal amplification electrochemical aptasensor based on Ag@Au core-shell nanoparticles was prepared by layer-by-layer method for the detection of $SM_2$. The constructed aptasensor showed favorable performance toward $SM_2$ detection due to the superior properties of Ag@Au core-shell including large surface area to elevate APT binding site, high biocompatibility to immobilize APT, and high conductivity to enhance the sensitivity of aptasensor. The method provides an efficient strategy for developing electrochemical aptasensor.

**Acknowledgments** This work was supported by the National Natural Science Foundation of China (Grant No. 61301037), the Cultivation Plan for Young Core Teachers in Universities of Henan Province (No. 2017GGJS072), the Henan Science and Technology Cooperation Project (Grant No. 172106000014), and the Youth Backbone Teacher Training Program of Henan University of Technology (Grant No. 21420004).

## Compliance with ethical standards

**Conflict of interest** The authors declare that they have no conflict of interest.

## References

1. Zhang Y, Weiqing LI, Zhou W, et al. Progress in sample pretreatment and analytical techniques for the determination of sulfonamide residues in foods. Food Sci. 2015.
2. Liu N, Danhong LI, Xing K, et al. Comparison of three pretreatment methods for the extraction of sulfadimidine in chicken breast meat. Chin J Bioprocess Eng. 2018.
3. Nevado JJB, Peñalvo GC, Bernardo FJG. Determination of sulfametoxazole, sulfadiazine and associated compounds in pharmaceutical preparations by capillary zone electrophoresis. J Chromatogr A. 2001;918:205–10.
4. Kaufmann A, Roth S, Ryser B, et al. Quantitative LC/MS-MS determination of sulfonamides and some other antibiotics in honey. J AOAC Int. 2002;85:853–60.
5. Ling LI, Zhao XL, Wang X, et al. Determination of sulfonamides in pork by molecular imprinted solid phase extraction combined with high performance liquid chromatography. Sci Technol Food Ind. 2017.
6. Li S, Zhao J, Wang W, et al. Simultaneous determination of ten sulfa drugs in chicken meat by high performance liquid chromatography-coulometric array detector. Chin J Anal Chem. 2005;33:442–6.
7. Zhang YY, Jin SP, Zi-Cheng LI, et al. Determination of sulfonamides in feed by capillary electrophoresis with electrochemical detection. Chin J Anal Lab. 2010;29:1–5.
8. He B, Du G. Novel electrochemical aptasensor for ultrasensitive detection of sulfadimidine based on covalently linked multiwalled carbon nanotubes and in situ synthesized gold nanoparticle composites. Anal Bioanal Chem. 2018;410:2901–10.
9. Duan J, Xing-Hua LI, Liu K, et al. Determination of sulfonamide residues in milk by high performance liquid chromatography-chemiluminescence method. Chin J Anal Chem. 2017.
10. Zhang Y, Xu X, Qi X, et al. Determination of sulfonamides in livers using matrix solid-phase dispersion extraction high-performance liquid chromatography. J Sep Sci. 2015;35:45–52.
11. Granja RH, Niño AM, Rabone F, et al. A reliable high-performance liquid chromatography with ultraviolet detection for the determination of sulfonamides in honey. Anal Chim Acta. 2008;613:116–9.
12. Assassi N, Tazerouti A, Canselier JP. Analysis of chlorinated, sulfochlorinated and sulfonamide derivatives of n-tetradecane by gas chromatography/mass spectrometry. J Chromatogr A. 2005;1071:71.
13. Reeves VB. Confirmation of multiple sulfonamide residues in bovine milk by gas chromatography-positive chemical ionization mass spectrometry. J Chromatogr B Biomed Sci Appl. 1999;723:127–37.
14. Pailler JY, Krein A, Pfister L, et al. Solid phase extraction coupled to liquid chromatography-tandem mass spectrometry analysis of sulfonamides, tetracyclines, analgesics and hormones in surface water and wastewater in Luxembourg. Sci Total Environ. 2009;407:4736–43.
15. Stoob K, Singer HP, Goetz CW, et al. Fully automated online solid phase extraction coupled directly to liquid chromatography-tandem mass spectrometry. J Chromatogr A. 2005;1097:138–47.

16. Santos B, Lista A, Simonet BM, et al. Screening and analytical confirmation of sulfonamide residues in milk by capillary electrophoresis-mass spectrometry. Electrophoresis. 2010;26: 1567–75.
17. Li Z, Li Y, Qi M, Zhong S, Wang W, Wang AJ. Graphene-$Fe_3O_4$ as a magnetic solid-phase extraction sorbent coupled to capillary electrophoresis for the determination of sulfonamides in milk. J Sep Sci. 2016;39:3818–47.
18. Luo YF, Wu L, Kong L, et al. A simple and rapid electrochemical method for detection of melamine in milk. Chem Sensors. 2013.
19. Zheng JY, Fang-Jing DU, Cai-Mei HE, et al. Electrochemical sensor for detection of bisphenol a incorporating aptamer. J Yanan Univ. 2018.
20. Dun-Ming XU, Min WU, Zou Y, et al. Application of aptamers in food safety. Chin J Anal Chem. 2011;39:925–33.
21. Zhao Y, Xie X, Zhao Y, et al. A novel electrochemical aptamer biosensor based on DNAzyme decorated Au@Ag core-shell nanoparticles for $Hg^{2+}$ determination. J Braz Chem Soc 2017.
22. Gondim CS, Durán GM, Contento AM, et al. Development and validation of an electrochemical screening methodology for sulfonamide residue control in milk samples using a graphene quantum dots@nafion modified glassy carbon electrode. Food Anal Method. 2018:1–11.
23. Peng H, Qi W, Li S. Modeling the phase stability of janus, core–shell, and alloyed Ag–Cu and Ag–Au nanoparticles. J Phys Chem C. 2015;119:2186–95.
24. Yang J, Lee JY. Core−shell Ag−Au nanoparticles from replacement reaction in organic medium. J Phys Chem B. 2005;109:19208.
25. Miao X, Zou S, Zhang H, et al. Highly sensitive carcinoembryonic antigen detection using Ag@Au core–shell nanoparticles and dynamic light scattering. Sensors Actuators B Chem. 2014;191:396–400.
26. Xin Z, Hui W, Su Z. Fabrication of Au@Ag core–shell nanoparticles using polyelectrolyte multilayers as nanoreactors. Langmuir. 2012;28:15705–12.
27. Hamidi-Asl E, Dardenne F, Pilehvar S, et al. Unique properties of core-shell Ag@Au nanoparticles for the aptasensing of bacterial cells. 2016;4:16.
28. Li N, Wang Y, Li Y, et al. A label-free electrochemical immunosensor based on Au@Pd/Ag yolk-bimetallic shell nanoparticles and amination graphene for detection of nuclear matrix protein 22. Sensors Actuators B Chem. 2014;202:67–73.
29. Tang D, Yuan R, Chai Y. Ligand-functionalized core/shell Ag@Au nanoparticles label-free amperometric immun-biosensor. Biotechnol Bioeng. 2006;94:996–1004.
30. Mao K, Yang Z, Li J, et al. A novel colorimetric biosensor based on non-aggregated Au@Ag core–shell nanoparticles for methamphetamine and cocaine detection. Talanta. 2017;175:338.
31. Singh P, Thuy NTB, Aoki Y, et al. Intensification of surface enhanced raman scattering of thiol-containing molecules using Ag@Au core@shell nanoparticles. J Appl Phys. 2011;109:1067.
32. Ung T, Mulvaney P, Liz-Marzan LM. Controlled method for silica coating of silver colloids. Influence of coating on the rate of chemical reactions. Langmuir. 1998;14:3740–8.
33. Meng HY, Wang X, Zhang B, et al. Signal enhanced electrochemical aptasensor for detection of $Hg^{2+}$ based on Au@Ag core-shell nanomaterial. Chi J Anal Lab. 2017.
34. Li C, Jiang Q, Physics DO, et al. Synthesis and optical properties of Au-Ag alloy nanoparticles and Ag@Au nanoparticles. Henan Sci. 2015.
35. Tabrizi MA, Shamsipur M, Sherkatkhameneh N. Flow injection amperometric sandwich-type electrochemical aptasensor for the determination of adenocarcinoma gastric cancer cell using aptamer-Au@Ag nanoparticles as labeled aptamer. Electrochim Acta. 2017.
36. Le T, Sun Q, Xie Y, et al. A highly sensitive aptasensor for sulfamethazine detection using an enzyme-linked aptamer assay. Food Anal Method. 2018:1–10.
37. Su YL, Cheng SH. A novel electroanalytical assay for sulfamethazine determination in food samples based on conducting polymer nanocomposite-modified electrodes. Talanta. 2018;180:81–9.